Determination of CaO carbonation kinetics under recarbonation conditions

G. Grasa*[a]; I. Martínez[a]; M.E. Diego[b], J.C. Abanades[b]

[a]*Instituto de Carboquímica (Consejo Superior de Investigaciones Científicas), Miguel Luesma Castán 4, 50018 Zaragoza (Spain)*

[b]*Instituto Nacional del Carbón (Consejo Superior de Investigaciones Científicas), Francisco Pintado Fé 26, 33011 Oviedo (Spain)*

emails: gga@icb.csic.es; imartinez@icb.csic.es; marlen@incar.csic.es; abanades@incar.csic.es

Abstract

This work investigates the kinetics of the reaction of CO_2 with CaO particles partially carbonated that are forced to increase their carbonate content at high temperatures in an atmosphere of rich CO_2. This additional recarbonation reaction, on particles that have already completed their fast carbonation stage, is the basis of a novel process that aims to increase the CO_2 carrying capacity of sorbents in Calcium looping CO_2 capture systems. The CaO reaction rates and the maximum carbonation conversions after the recarbonation step were measured on a thermogravimetric analyzer and the results indicate that they are highly dependent on temperature and CO_2 partial pressure, steam also being a contributing factor. The reaction mechanism governing the reaction rates during the carbonation and recarbonation reactions is explained by the combined control of chemical reaction and CO_2 diffusion through the $CaCO_3$ product layer. An extension of the Random Pore Model adapted to multi cycled CaO particles was successfully applied to calculate the CaO molar conversion as a function of time and the recarbonation conditions, using kinetic parameters consistent with previous published results on carbonation kinetics under typical flue gas conditions.

KEY WORDS: CO_2 capture, regenerable sorbents, carbonation, CO_2 carrying capacity kinetics, limestone

Introduction

CO_2 capture and storage, CCS, is a major mitigation option for addressing the problem of climate change and there is a range of mature CO_2 capture technologies that could be rapidly deployed if the right incentives were in place[1]. The potential for reducing costs in optimized plants with already existing CO_2 capture technologies is important. However, a number of emerging CO_2 capture technologies may offer much deeper cost savings[1].

Among these emerging technologies is the Post-combustion Calcium looping process, CaL, which is based on the carbonation reaction of CaO and CO_2. It has experienced rapid growth in recent years from a mere concept (first proposed by Shimizu et al.[2]) to small scale pilot demonstration of interconnected reactors [3-7] and more recently to larger scale pilots[8, 9, 10] of up to 1.7 MW_{th}[11, 12]. In a typical CaL system, the CaO particles react with the CO_2 contained in the flue gas in the carbonator unit, which operates at high temperature (650-700 ºC) to form $CaCO_3$. This carbonate is calcined by the oxy-combustion of coal at temperatures of around 880-910ºC in a second circulating fluidized bed, the calciner (see Figure 1). The high temperature gas and solids streams allow an efficient heat recovery that can be integrated with a steam cycle to generate additional power[13-16]. In this way the energy penalty associated with the capture process is reduced to 6-7 net points assuming standard equipment in the Air Separation Unit, ASU, required for oxy-combustion, and in the CO_2 compression and purification unit, CPU. Any improvement in the ASU or CPU elements of the oxy-fuel combustion systems will also benefit the CaL system as the

consumption of O_2 in the calciner still remains the main energy penalty in the process and a major cost component.

A well-known drawback of all CaL technologies is the decay in the CO_2 carrying capacity that the sorbent experiences with the number of calcination/carbonation cycles[17-21]. The low cost and availability of the raw limestone material used in CaL systems allows a sufficiently large make-up flow of limestone to compensate for the decay in activity, making it possible to purge the system of ashes and $CaSO_4$. It is, however, important for the development of large scale CaL technology to be able to operate with a minimum sorbent requirement and maximum sorbent stability[21-23]. For this reason, intensive research is being carried out to find ways to reactivate CaO materials and to obtain more stable CaO-based sorbents, as explained in recent reviews by Anthony[24] and Blamey et al[25].

Recently, our group proposed[26] a novel process to increase and stabilize the CO_2 carrying capacity of CaO particles in a CaL system. This is achieved by including a short recarbonation stage between the carbonator and the calciner, in which highly carbonated particles from the carbonator are forced to increase their conversion to slightly above their 'maximum carrying capacity' (usually signaled by the end of the fast carbonation period under normal carbonation conditions). The fundamentals of the process are based on the ability of CaO to react with CO_2 up to conversions over 80% after ten cycles of 24 hours in pure CO_2 as shown by Barker[18]. More recent experimental studies have revealed that extended carbonation times (up to 30 minutes) lead to sorbents exhibiting greater residual activity[27, 28] with respect to the activity of solid sorbents subjected to shorter reaction times[29]. Similar results were found with sorbents tested under higher CO_2 partial pressure[30,31]. Also the use of pure CO_2 and long carbonation reaction times, was

investigated as a method to increase CO_2 carrying capacities, but contradictory results at TGA and fluidized bed lab scale[32] were obtained.

The recarbonation process proposed in this study includes a new reaction step carried out in a separate reactor (the recarbonator in Figure 1) where the partially carbonated stream of solids exiting the carbonator unit is placed in contact with a highly concentrated CO_2 stream at high temperature (generated in the calciner unit). The purpose of this is to produce an additional conversion of the solids under the slow reaction regime in order to achieve an increase in the carbonate conversion that will compensate for the decay in the CO_2 capture capacity the solids will undergo the next time they pass through the calciner and carbonator[26].

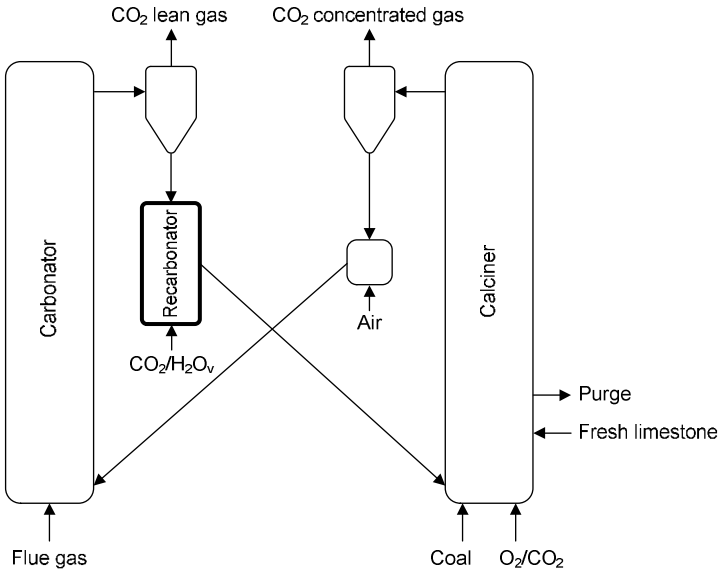

Figure 1. Block diagram of a CaL system including a recarbonator reactor.

It is well known that the ability of CaO to react with CO_2 in the slow reaction regime has little impact on the CO_2 carrying capacity of the sorbent under the standard carbonation conditions in a CaL system. This is because the average residence times of the solids in the

carbonator reactor amount to only a few minutes[6, 7] for typical solids inventories and circulation flows. Besides, the average CO_2 partial pressures around the particles in the reactor are well below 15 kPa when the CO_2 capture efficiency is high. However, the sorbent may be reacting sufficiently fast under the enhanced carbonation conditions of the recarbonator reactor in Figure 1. The recarbonation process in Figure 1 opens up a new scenario for the study of carbonation reaction kinetics on the basis of the ability of CaO particles that are already partially carbonated to continue reacting with CO_2 at the high temperatures and CO_2 partial pressures present in the recarbonator reactor. Evaluation of the reaction kinetics in the slow reaction regime at a higher temperature and pCO_2 will be critical for the design of the recarbonator reactor. A substantial background of literature exists on the relevant kinetics and mechanism of reaction between CaO and CO_2, as reviewed in the following paragraphs.

Early experimental studies of the carbonation kinetics of CaO revealed the existence of two stages in the carbonation reaction rates [2, 18, 19, 21, 33, 34]: a fast chemically controlled initial reaction stage and a second slower reaction stage controlled mainly by the diffusion of CO_2 through the product layer. Various models based on sorbent structural properties have been used in the literature to describe in detail the kinetics of these two reaction regimes, as compiled in the review by Stanmore and Gillot[35], and they can be classified into grain models or pore models. The grain models for CaO carbonation see the particle as a porous structure consisting of a grain matrix formed as a result of the previous calcination step[36-38]. The size of the CaO grains determines to a large extent the amount of active surface for reaction. Stendardo and Foscolo[37] assumed an average grain size, with a uniform dispersion of CaO grains that are gradually transformed into $CaCO_3$. Bouquet et al[36] applied a

micrograin-grain model that distinguishes three differentiated reaction stages during the filling of all the voids present in the CaO micrograins. During this void-filling process the shrinking core model applied to the micrograin showed that there is a short kinetically controlled regime, followed by a combined control by chemical reaction and diffusion through the carbonate layer. Finally the CO_2 diffuses at the grain level through the carbonate to reach the inner CaO cores. A second group of researchers applied pore models that take into account the evolution of the pore size distribution of the sorbent during the carbonation reaction[33, 39]. The Random Pore Model, RPM, developed by Bhatia[33] considered the pore structure as a network of randomly interconnected pores, and defined the key particle structural parameters on the basis of this geometry. They developed a general expression for the instantaneous gas-solids local reaction rate applicable to porous systems in the presence of a product layer diffusion resistance.

Sun et al[39] developed a new gas-solid model for the carbonation of CaO based on discrete pore size distribution measurements. This model uses the initial pore size distribution of the lime resulting from calcination of the fresh limestone as input data. The only fitting parameter used was the effective diffusivity through the product layer (which was also dependent on the evolution of the pore system).

As mentioned above, the carbonation reaction shows an abrupt change from the chemical to the diffusional controlled regime, which has been generally attributed to the formation of a $CaCO_3$ product layer on the free CaO reaction surface [18, 20, 21, 29, 33, 36, 39-42]. Alvarez and Abanades[40] have established that the product layer thickness representing the transition between the fast and the slow reaction regimes for reaction conditions of practical interest for CaL systems, is around 50 nm. Using a simple pore model to interpret the data

obtained from Hg porosimetry measurements, they described the progression of the carbonation reaction on the CaO surface as the filling of the available rich porous structure of the calcined material. Once the small pores and part of the large voids are covered with a $CaCO_3$ layer of around 50 nm CO_2 diffusion is restricted, and this causes a slower conversion of the solids. Bouquet et al[36] proposed that the transition between diffusion resistance at micrograin to grain level starts once the voids between micrograins are filled with a $CaCO_3$ layer of around 43 nm. The scale of diffusion at grain level is responsible for the drastic decay in the reaction rate, and the diffusion coefficient through the product layer decreases upon the formation of carbonate. Mess et al[34] described the growth of the product layer as a coalescence phenomenon, in which the grain growth is highly dependent on temperature. The effective diffusion coefficient is expressed as a combination of the grain boundary diffusion coefficient and the bulk diffusion coefficient through the product layer and is dependent on the conversion of solids, as the grain boundary length diminishes while the product layer becomes more developed. The effective diffusion coefficient decreases with the conversion of solids. The increasing resistance of CO_2 diffusion with increasing $CaCO_3$ content has also been noted by Stendardo and Foscolo[37] to fit the experimental carbonation conversion curves of calcined dolomite in their spherical grain model. Sun et al[39] related the diffusion coefficient to the evolution of the pore system.

In contrast with these variable effective diffusion coefficients, Bhatia and Perlmutter[33] assumed a homogeneous product layer with a single diffusion coefficient only dependent on temperature to describe the diffusion process.

Recent studies on the effect of temperature on the carbonation reaction of CaO under the diffusion reaction regime have shown that the reaction kinetics are improved when the reaction temperature is increased in what appears to be another fast reaction regime[43]. These findings reinforce the relation of the diffusion coefficient with temperature, and show that the contribution of the CO_2 diffusion resistance through the product layer to the total reaction rate is highly determined by reaction temperature. Also, according to the detailed observations and modelling work of Li et al.[43], the morphology of the product layer is largely dependent on the reaction temperature. When the reaction temperature is increased, the thickness of the islands those initially form the $CaCO_3$ layer increases while their density over the CaO surface diminishes leaving, for a given level of conversion, a higher fraction of free CaO surface for chemically controlled reaction. This is a critical piece of information for understanding and interpreting the experimental results presented in this work.

The objective of this paper is to extend the scope of the experimental results available in order to model the carbonation reaction in the different stages of the system of Figure 1 and, in particular, to determine the effect of the main operating variables (i.e., the reaction temperature, the CO_2 partial pressure and the presence of steam) upon the conversion achieved by CaO particles under recarbonation conditions. The kinetic parameters that govern the reaction in the new reaction conditions will be determined using the Random Pore Model. A second objective of the paper is to reinforce the experimental evidence of the positive effects of the recarbonation step on the increase in the residual CO_2 carrying capacities of CaO particles.

Experimental

A Spanish limestone, Compostilla presenting 93.04 wt% of CaO (and main impurities Fe_2O_3 2.5%wt., MgO 0.76 %wt., K_2O 0.46% wt., SiO_2 0.33 %wt. and TiO_2 0.37% wt.), was used in the experimental tests to determine the principal variables affecting the carbonation reaction under recarbonation conditions. Most experiments were carried out with samples with a narrow particle size interval (75-125 micron) that were texturally characterized by using a Hg Porosimeter Quantachrome Pore Master to estimate the pore volume and the pore-size distribution. N_2 adsorption (Micromeritics ASAP2020) at 77 K was used to calculate the surface area by applying the Brunauer, Emmett and Teller equation to the adsorption isotherm.

The experimental tests were carried out on a TGA apparatus that has been described in detail in previous papers[41]. Briefly, the reactor consists of a quartz tube with a platinum basket suspended from it, inside a two-zone furnace. The furnace can be moved up and down by means of a pneumatic piston. The position of the furnace with respect to the platinum basket allows alternation between calcination and carbonation conditions. The temperature and sample weight were continuously recorded on a computer. The reacting gas mixture (CO_2, O_2/air) was regulated by mass flow controllers and fed in through the bottom of the quartz tube. Steam was generated by external electric heating of the water flow controlled by a liquid mass flow controller and then introduced into the reaction atmosphere for some specific tests.

The materials used to determine the reaction kinetics of the carbonation reaction under recarbonation conditions (elevated reaction temperature and CO_2 partial pressure) were partially deactivated CaO particles, with an average CO_2 carrying capacity of between 0.15 and 0.30 CaO molar conversion, which is representative of the activity of the average

material circulating in a large-scale CaL system. To prepare this material, batches of around 150 mg of limestone were placed inside a platinum pan in the TGA apparatus and subjected to relatively standard calcination/carbonation cycles (the calcination of the sample was carried out at 875 ºC in air for 30 min and the carbonation was carried out at 650 ºC in 5 kPa CO_2 in air for 30 minutes to ensure full saturation of the sorbent up to its maximum carrying capacity, X_N). The solids prepared by this procedure had been subjected to the recarbonation tests described below.

Three mg of partially deactivated sorbent was placed in the TGA pan in each individual kinetic test, and the total gas flow was set to $4*10^{-6}$ m^3/s to eliminate external diffusion resistances to the reaction[41]. To avoid any effect associated with the preparation of the samples that might interfere with the interpretation of the experimental results, every recarbonation test involved several standard calcination/carbonation cycles at the beginning of each test. The routine of the standard cycles was: calcination at 875 ºC in air for 5 minutes followed by carbonation at 650 ºC in 5 kPa CO_2 in air for 5 minutes. After several cycles under these standard conditions a recarbonation stage was added to the routine just after the end of the carbonation stage of the solids. The effect that the recarbonation temperature (between 700 and 800 ºC) and the pCO_2 in the reaction atmosphere (between 60 to 100 kPa CO_2) had on the carbonation reaction kinetics under recarbonation conditions was experimentally evaluated. The presence of steam during recarbonation was tested by including 15%v of steam in the CO_2 atmosphere in some specific tests. Some standard carbonation/calcination tests were also carried out to test whether the sorbent carbonation kinetic parameters were in agreement with the values presented in the literature for the CaO carbonation reaction.

Furthermore, to determine the impact that the recarbonation stage has on sorbent residual activity, around 10 mg of limestone sample was subjected to 75 repeated calcination/carbonation cycles according to the following routine: calcination of the sample at 875 ºC in air for 5 minutes, carbonation at 650 ºC in 5 kPa CO_2 in air for 5 min and recarbonation in pure CO_2 for 5 minutes. The tests were carried out at recarbonation temperatures of 700 and 800 ºC. For comparison purposes, the same material was also tested under a "typical" calcination-carbonation experimental routine without any recarbonation step (calcination at 875ºC in air for 5 minutes and carbonation at 650ºC in 5 kPa CO_2 in air for 5 minutes).

Results and discussion

Figure 2 provides an example of the experimental results that illustrate the positive effect of the recarbonation step on the CO_2 maximum carrying capacity $X_{N,R}$, achieved by the sorbent at the end of the fast reaction period of the carbonation reaction and after several calcination-carbonation-recarbonation cycles. Two types of curve appear in this plot of the carbonate CaO conversion vs. time: a grey line corresponding to the reference carbonation test conducted without recarbonation (after 17 standard cycles of calcination-carbonation), and a black line corresponding to the carbonation and recarbonation test conducted after 15 standard cycles and 2 additional cycles of calcination-carbonation-recarbonation stages. According to the nomenclature in Figure 2, N corresponds to the total number of calcinations experienced by the sample (17 in this case) and R corresponds to the number of recarbonation stages (2 in the example of Figure 2).

This second curve has two clearly separate reaction stages under different reaction conditions. During the initial ~280 s, the sorbent is reacting under typical carbonation conditions (650 ºC and 5 kPa CO_2 in air, as in the case of the grey curve used as a reference) and the CaO conversion vs. time curve shows a typical fast carbonation stage (which lasts for about 60-70 seconds in these conditions) controlled by the chemical reaction, followed by a slower reaction stage controlled by the combined resistance of the chemical reaction and CO_2 diffusion through the product layer[33, 41] although diffusion is the predominant resistance. The slow reaction period leads very rapidly to a characteristic stage of conversion, X_N (without recarbonation) or $X_{N,R}$ (with recarbonation), as shown in Figure 2, which corresponds to the maximum CO_2 carrying capacity of the sorbent for each cycle number N on both curves. After 280s of carbonation, the reaction conditions remain unchanged in the reference experiment without recarbonation, but they switched over to the conditions required by the recarbonator reactor in Figure 1 (in this particular test: 800 ºC and 85 kPa CO_2) in the black curve.

As it can be seen, thanks to the recarbonation stage, the CO_2 carrying capacity of the reactivated sorbent, $X_{N,R}$, has noticeably increased with respect to the reference value, X_N, for an identical number of calcination cycles. Furthermore, the slope of the initial fast reaction stage (chemically controlled) and the second slower reaction stage controlled by the diffusion are almost identical for the reactivated and the non-reactivated curves under the carbonator operating conditions (first 280 s). This suggests that the kinetic constants and the diffusion parameters from the carbonation reaction rate expressions have not been affected very much by the inclusion of the recarbonation stage. Therefore, the cause of the

rapid increase in carbonate conversion during recarbonation, ΔX_R, must be the change in the reaction temperature and the CO_2 partial pressure.

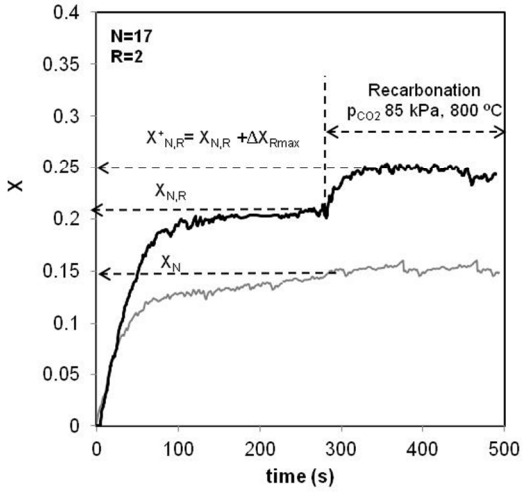

Figure 2. Example of the experimental carbonation and recarbonation CaO conversion curves after 17 calcination cycles (N=17 in both curves). The black curve is obtained after 15 standard cycles of calcination-carbonation and 2 cycles of calcination-carbonation-recarbonation (R=2). Calcination at 875 ºC in air. Carbonation at 650 ºC and 5 kPa CO_2 in air. Recarbonation at 800 ºC and 85 kPa CO_2 in air.

As can be seen in Figure 2, once the experimental conditions have been switched over to the recarbonation conditions the slope of the CaO conversion curves increases with respect to the slope of the diffusion regime at lower temperature until X reaches a new plateau, $X^+_{N,R=} X_{N,R} +\Delta X_{R,max}$, in which the reaction rate slows down again. These experimental CaO conversion curves which incorporate the gain in conversion during recarbonation, $\Delta X_{R,max}$, can be used to derive the kinetic parameters for the recarbonation reaction stage. As pointed out above a series of experiments were carried out to evaluate the effect of the

reaction temperature, the CO_2 partial pressure and the presence of steam upon the recarbonation rates of CaO partially converted to $CaCO_3$ in the preceding reaction period at standard carbonation conditions.

Figure 3 shows experimental conversion curves in which the recarbonation temperature was 750º and 700 ºC respectively (under 85 kPa CO_2 in air). As can be seen, from a comparison of the experimental results of Figures 2 and 3, the $\Delta X_{R,max}$ achieved under recarbonation conditions is greatly affected by temperature. In the series of Figure 2, carried out at 800 ºC, the sorbent is able to achieve ≈0.04 additional conversion points in the space of 60 s, while the slope of the CaO conversion curve under recarbonation is less steep at lower temperatures and the value of $\Delta X_{R,max}$ is consequently smaller at the end of the recarbonation time fixed for this experiment. The presence of this plateau at which the carbonation reaction rate is extremely slow even under recarbonation conditions was also confirmed at these lower temperatures in other experiments with longer recarbonation times.

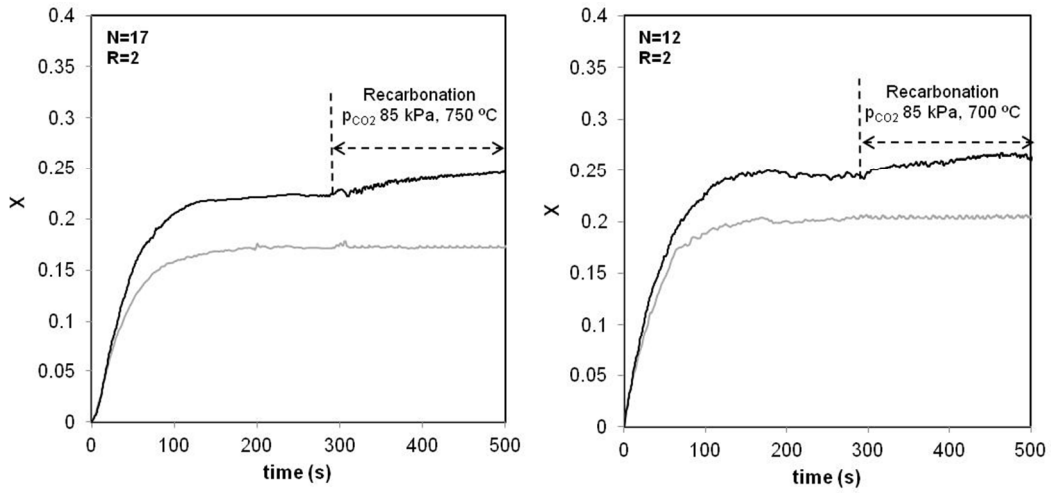

Figure 3. Experimental carbonation and recarbonation CaO conversion curves for two different recarbonation temperatures: left) 750 ºC, and right) 700ºC. Calcination and carbonation conditions as in Figure 2.

The presence of this second plateau in the conversion of CaO supports recent mechanistic studies by Li at al[43] who claim that temperature affects the rate of growth of the carbonate product layer that forms over the entire surface of the CaO particles. The growth of the carbonate layer has been described as a coalescence phenomenon of $CaCO_3$ islands[34, 43], so that once the islands of $CaCO_3$ cover the whole of the CaO surface and reach a critical thickness, CO_2 diffusion through the $CaCO_3$ layer is severely hindered. The island growth rate has been directly related to temperature[34], as have the characteristic island dimension[43].

To analyze the effect of the reaction atmosphere on the kinetics of the recarbonation reaction several tests were carried out at 800ºC, in which the pCO_2 in the reaction atmosphere was varied from 60 to 100 kPa CO_2. As can be seen in Figure 4 left), the reaction rate under recarbonation conditions increases with increasing CO_2 concentration. However, the CaO conversion that marks the onset of the second plateau is independent of the CO_2 partial pressure, and from this point the reaction rate is independent (and very slow) of CO_2 partial pressure. This is in agreement with the expression formulated by Bhatia and Perlmutter for pure diffusion control[33].

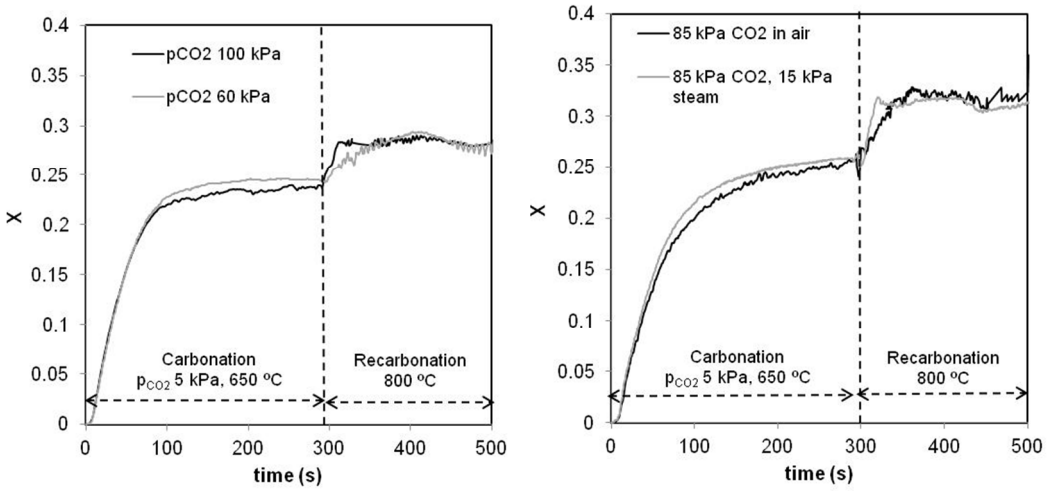

Figure 4. Left) Effect of the CO_2 partial pressure on CaO conversion during recarbonation at 800 ºC, N=12 and R=2. Right) Effect of the presence of steam on CaO conversion during recarbonation at 800 ºC and 85 kPa CO_2, N=12 and R=2. Calcination and carbonation conditions as in Figure 2.

The effect that the presence of steam has on the recarbonation reaction was evaluated by carrying out a series of tests with 15%v steam in CO_2. The steam was added only during the recarbonation stage. The results presented in Figure 4 right) correspond to two experiments carried out using a similar procedure with and without steam. After 10 standard calcination-carbonation cycles, several cycles including a recarbonation stage were carried out. The series presented correspond to samples that experienced 12 calcinations (N=12) and 2 recarbonations (R=2) with the presence of steam (grey line) and without steam (black line). The experimental results show that the slope of the CaO conversion curve during recarbonation in the presence of steam is around 1.5 times larger than the slope of the conversion curve without steam. This qualitative trend was also observed in other similar experiments with steam and indicates that the reaction rate during recarbonation increases in the presence of steam, which is in agreement with experimental

results compiled in the literature from which it can be concluded that diffusion resistance is diminished in the presence of steam[44, 45].

To fit the experimental conversion data vs. time we have used the Random Pore Model[33], that has been adapted in order to model the carbonation reaction of sorbents that have experienced multiple calcination/carbonation cycles[41]. The main novelty of this adapted version of the RPM is the estimation of the sorbent structural parameters included in the model equations (S, L, ε and Ψ) from the textural properties of the sorbent resulting from the calcination of the fresh limestone and the evolution of the CaO conversion with the number of cycles. To predict the evolution of the CaO conversion with time (experimental curves plotted in Figures 2, 3 and 4) the general expression of the reaction rate can be integrated, taking into account the different controlling mechanisms: chemical reaction kinetic control, and combined control by the reaction and diffusion through the product layer. There is also a third controlling mechanism, pure diffusion control, but in this case the particles experience almost no increase in their carbonate content. From the previous experimental curves it can be seen that the fast reaction stage of the carbonation reaction is controlled by the chemical reaction, and according to the model proposed by Grasa et al.[41], the abrupt change to the slower reaction rate under carbonation conditions is determined by the formation of a product layer thickness of around 40 nm (the conversion associated with this layer thickness is referred to as X_{KD} in Grasa et al.[41]). Equation (1) can be applied to predict the evolution of the CaO conversion with time under the chemically controlled regime, where Ψ is the sorbent structural parameter and τ is the non dimensional time[41]:

$$X = 1 - exp\left(\frac{1-\left(\frac{\tau}{2}\Psi+1\right)^2}{\Psi}\right) \qquad \text{for } X \leq X_{KD} \qquad (1)$$

Once the fast reaction stage has finished, from X_{KD} onwards, the reaction can be modeled as combined control by the chemical reaction and diffusion but with the predominant control of diffusion phenomena through the product layer. These will be the phenomena that control the carbonation reaction when the sorbent particles initiate a recarbonation reaction period, since they present a CaO conversion close to $X_{N,R}$ (see Figure 2). Equation (2) can be applied to predict the CaO carbonation conversion under this hypothesis of combined control until the sorbent reaches the conversion associated with the end of the fast recarbonation period, $X^{+}_{N,R}$ (see Figure 2).

$$X = X_{KD} + \left(1 - \exp\left(\frac{1}{\Psi} - \frac{\left[\sqrt{1+\beta Z\tau} - \left(1-\frac{\beta Z}{\Psi}\right)\right]^2 \Psi}{\beta^2 Z^2}\right)\right) \text{ for } X_{KD}<X<X^{+}_{N,R} \qquad (2)$$

Finally, a second dramatic decrease in reaction rate appears on the experimental CaO conversion curves, once the sorbent reaches $X^{+}_{N,R}$. From this point onwards the conversion rate of CaO is very slow, and the change in the mechanism that controls the carbonation reaction from combined control by the chemical reaction and diffusion to pure diffusional control might explain this decrease in the reaction rate. According to the experimental results, the evolution of the CaO conversion with time after $X^{+}_{N,R}$ is independent of the CO_2 partial pressure, which is consistent with a pure diffusion-controlled reaction regime[33].

The previous experimental results and the mechanism proposed in the literature[36, 40, 41], indicate the importance of the experimental determination of the critical carbonate layer thickness on the free surfaces of CaO for establishing the transition between the different reaction regimes. For the new transition, when $X^{+}_{N,R}$ is reached and the reaction rate becomes negligible, the product layer thickness h_D can be estimated as follows:

$$h_D = \frac{(X^+_{N,R} V^M_{CaCO3} \rho_{CaO})}{S_{N,R,} M_{CaO}} \quad (3)$$

where $S_{N,R}$ is the reaction surface at cycle N, calculated as the product of the reaction surface of the resulting from the calcination of the fresh limestone and the conversion at the end of the carbonation cycle after N calcinations and R recarbonations ($X_{N,R}$), $V_{CaCO3}{}^M$ is the carbonate molar volume, ρ_{CaO} is the CaO true density and M_{CaO} is the CaO molar weight. A consistent value of $CaCO_3$ product layer thickness, h_D, of 70 nm has been estimated from the experimental data presented in Figures 2 and 4 for recarbonations carried out at 800 ºC.

The sorbent kinetic parameters, i.e., the chemical reaction constant, k_s, and the effective product layer diffusion coefficient, D, were determined from the experimental CaO conversion curves with the aid of the RPM model at different temperatures, as described in Grasa et al.[41]. Both parameters have been expressed in the form of Arrhenius expressions, and the values obtained for the pre-exponential factors (k_{so} and D_o) and for the activation energies (E_{aK} and E_{aD}) are presented in Table 1 together with the limestone textural and structural parameters that were measured experimentally.

Table 1. Structural and kinetic parameters resulting from the calcination of the fresh limestone.

Structural Parameters		Kinetic Parameters	
S (m^2/m^3)	$34.22*10^6$	k_{so} (m^4/kmols)	$0.335*10^{-5}$
L (m/m^3)	$2.94*10^{14}$	E_{aK} (kJ/mol)	21.3
ε	0.37	D_o (m^2/s)	$3.37*10^{-5}$
Ψ	1.98	E_{aD} (kJ/mol)	140

The activation energies obtained for both the chemical reaction kinetic constant and the diffusion coefficient through the product layer are in close agreement with the values reported in the literature for the carbonation reaction of cycled CaO particles from natural limestone. The chemical reaction shows a lower dependence on temperature, as indicated by the typically low values of E_{aK}[33, 41, 42]. In contrast, the diffusion coefficient shows a high dependence on the temperature, as indicated by the high activation energies reported in the literature[33, 34, 41] and also found in this work. It should be noted that neither the pre-exponential factors nor the activation energies of the chemical reaction constant and the diffusion coefficient vary at any point along the conversion curves. Therefore, it must be the different reaction environment (in terms of temperature and CO_2 partial pressure) that is responsible for the variation in the reaction rate and the final conversions achieved during the recarbonation period. The ability of the RPM model to fit, with reasonable accuracy, such a wide variety of materials and operating conditions is a further validation of the general character of the model.

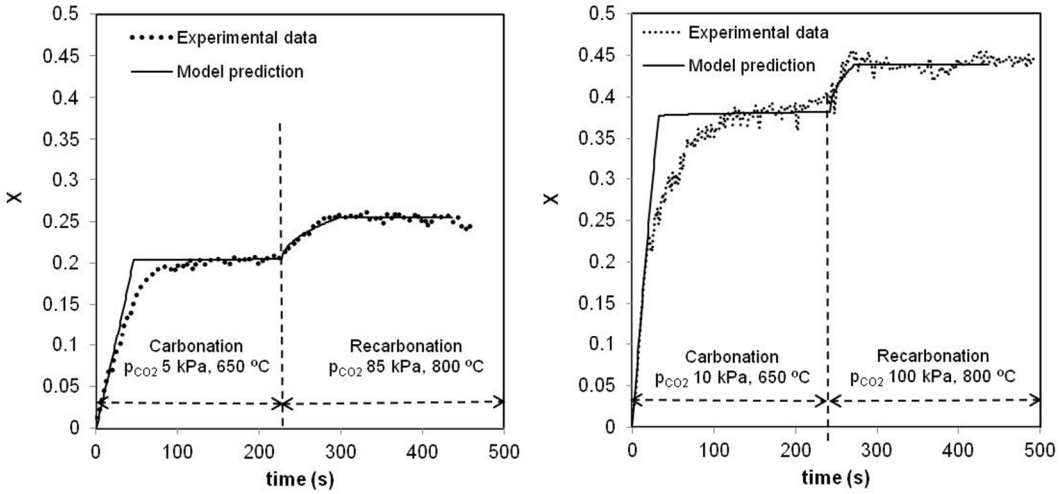

Figure 5. Comparison of the experimental data with the RPM model predicted values using the parameters of Table 1. Left) Carbonation at 650 ºCand 5 kPa CO_2 in air, and recarbonation at 800 ºC and 85 kPa CO_2 in air, N=17, R=2. Right) Carbonation at 650 ºC and 10 kPa CO_2 in air, and recarbonation at 800 ºC and 100 kPa CO_2 N=7, R=2.

Figure 5 shows that the model proposed successfully fits the evolution of the CaO conversion with time under both carbonation and recarbonation conditions. As can be seen the model predicts with sufficient accuracy the conversion curve of samples with a different CO_2 carrying capacity and also under different reaction conditions (in terms of temperature and CO_2 partial pressure). However, in order to integrate the previous reaction rate expression in recarbonator reactor models using the system of Figure 1, a simplified kinetic expression is derived from the experimental conversion curves, taking into account the relative modest gains in conversion during recarbonation. By analogy with previous works on modelling the carbonator reactor [41, 46, 47,48, 49] the reaction rate during the recarbonation

period is assumed to be constant from $X_{N,R}$ up to $X^{+}_{N,R}$. The CaO reaction surface available for reaction in the recarbonator reactor ($S_{N,Rav}$) can then be expressed as:

$$S_{N,Rav} = \frac{\Delta X_{R,max}\frac{\rho_{CaO}}{PM_{CaO}}}{(h_D - h_{max})\frac{\rho_{CaCO3}}{PM_{CaCO3}}} \quad (4)$$

where $\Delta X_{R,max}$ is the maximum conversion achievable in the recarbonator reactor, ρ_{CaO} and ρ_{CaCO3} are the densities of CaO and $CaCO_3$ respectively, PM_{CaO} and PM_{CaCO3} are the molecular weights of CaO and $CaCO_3$ respectively, h_{max} is the product layer thickness at the end of the fast reaction period in the carbonator (estimated as 40 nm according to Grasa et al.[41]) and h_D (70 nm according to the experimental results presented above) is the thickness of $CaCO_3$ which marks the end of the fast reaction stage in the recarbonator. In these conditions, the reaction rate can be expressed as:

$$\frac{dX}{dt} = k_{s,R} S_{N,Rav}\left(C_{CO2} - C_{eq}\right) \qquad \text{for } X_{N,R} < X < X^{+}_{N,R} \quad (5)$$

This expression is a simplification of the grain model expression[46, 50] successfully applied in previous works. The experimental values for $k_{s,R}$ obtained in the present work ranged from $3.5*10^{-8}$ and $4.0*10^{-9}$ (m^4/kmol s) for the series carried out at 800 ºC and 700 ºC respectively and at 85 kPa CO_2, from which the constant pre-exponential factor and the activation energy were derived (see Table 2). Also, by analogy with the approach adopted for the carbonator reactor models described in the literature[7, 46], the reaction rate expression can be represented as follows:

$$\frac{dX}{dt} = k_{s,R} X_{N,R}\left(\vartheta_{CO2} - \vartheta_{eq}\right) \qquad \text{for } X_{N,R} < X < X^{+}_{N,R} \quad (6)$$

where ϑ_{CO2} and ϑ_{eq} represent the CO_2 volume fraction in the gas phase and according to the equilibrium, respectively. According to this expression $k_{s,R}$ will be between 0.0044 s^{-1} for the series carried out at 800 ºC and 0.0005 s^{-1} for the experiments conducted at 700 ºC.

Table 2 also includes the kinetic parameters obtained from the experiments carried out in the presence of steam. As mentioned above, the presence of steam increases the conversion reaction rate, with the kinetic constant ranging according to Equation (5) between $7.6*10^{-8}$ at 800ºC and $5.6*10^{-9}$ (m^4/kmols) at 700 ºC.

Table 2. Kinetic parameters for the recarbonation reaction according to Equations (5) and (6) also included the values obtained in the presence of steam.

Kinetic parameters Eq. (5)		**Kinetic parameters Eq. (5) in presence of steam**		**Kinetic parameters Eq. (6)**		**Kinetic parameters Eq. (6) in presence of steam**	
$k_{s0,R}$ (m^4/kmols)	$10.5*10^3$	$k_{s0,R}$ (m^4/kmols)	$14*10^3$	$k_{s0,R}$ (s^{-1})	$28*10^6$	$k_{s0,R}$ (s^{-1})	$40*10^6$
E_{aR} (kJ/mol)	230	E_{aR} (kJ/mol)	230	E_{aR} (kJ/mol)	200	E_{aR} (kJ/mol)	200

Finally in order to gain a general overview of the impact of the recarbonation stage on the general CO_2 carrying capacity curves as a function of the number of carbonation-calcination cycles, several long duration series (75 cycles each) were conducted using three different recarbonation temperatures. Figure 6 shows the evolution of the CO_2 carrying capacity at the end of the fast carbonation period, $X_{N,R}$, against the number of calcination/carbonation cycles, N. For comparison, the Figure includes the typical standard sorbent decay curve (X_N vs. N) obtained for the carbonation reaction at 650ºC and 5 kPa CO_2 for 5 minutes (series with bold symbols). The two other experimental series

correspond to tests where the recarbonation step was carried out at 700 ºC and 800 ºC in pure CO_2 for 5 minutes. The experimental data were fitted to the typical expression from Equation (7) of X_N vs. N[29] and the derived parameters k and X_r that are compiled in Table 3 represent the deactivation constant and the residual capture capacity of the particles, respectively.

$$X_N = \frac{1}{\left(\frac{1}{(1-X_r)}+kN\right)} + X_r \qquad (7)$$

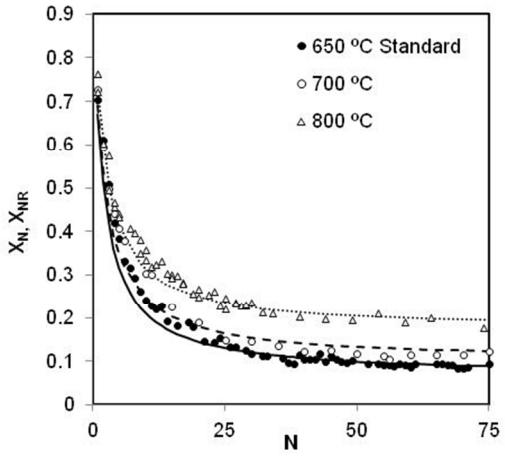

Figure 6. Evolution of X_N (black dots) and X_{NR} (void symbols) versus the number of calcination cycles for two different temperatures of recarbonation. Carbonation at 650ºC in all cases under 5 kPa CO_2, calcination at 875 ºC in air and recarbonation in pure CO_2 during 5 minutes after each carbonation.

Table 3. Sorbent deactivation parameters from the expression X_N vs N.

	k	X_r
650 ºC Standard	0.58	0.065

Recarbonated at 700 ºC in pure CO_2	0.58	0.10
Recarbonated at 800 ºC in pure CO_2	0.58	0.17

X_r was selected as the only fitting parameter for the series at high temperatures and CO_2 partial pressures to help in the interpretation of results. The sorbent in the series at 650ºC displays values of X_r that can be considered as the sorbent intrinsic deactivation parameters[31] and that are in close agreement with values reported in the literature for natural limestone and similar reaction conditions[29]. When a recarbonation stage is introduced into the experimental routine, the conversion under the diffusion controlled regime makes a more important contribution to the total sorbent conversion. This is in agreement with the predictions of the model by Arias et al[31] and with the experimental data, widely reported in the literature[18, 21, 27-29]. This confirms that the addition of a recarbonation reaction stage after each calcination-carbonation cycle (see Figure 1) could help to counteract the deactivation of naturally derived CaO materials used in postcombustion CO_2 capture systems based on Calcium Looping.

Conclusions

This work has experimentally confirmed that the introduction of a short (100-200 s) recarbonation stage on partially carbonated particles of CaO allows for the stabilization of sorbent carrying capacities at 0.15-0.20 molar conversion. High recarbonation temperatures (ideally between 750 and 800ºC), high partial pressures of CO_2 (over 60 kPa) and a certain presence of steam strongly favor the recarbonation reaction of CaO, reacting with CO_2 mainly in the slow diffusion reaction regime.

The Random Pore Model can be successfully adapted to multi-cycled particles to calculate the CaO molar conversion as a function of time and recarbonation conditions. The kinetic parameters needed to fit the recarbonation conversion curves are the same as those used to model the carbonation rates under normal carbonation conditions for the same sorbent

(k_{so} 0.335*10^{-5} m^4/kmols, E_{aK} 21.3kJ/mol; D_o 3.37*$10^{-5}$$m^2$/s, E_{aD} 140kJ/mol) which are also consistent with those published in previous works . This provides further validation of the RPM model as being suitable for a much wider range of carbonation and recarbonation conditions. However, the modest recarbonation conversions achieved in each cycle also allow the reaction to be modeled with simpler approaches with apparent reactions parameters that may be suitable for more general reactor models.

Notation

$C_{CO2,\,eq}$ concentration of CO_2 (kmol/m^3) at equilibrium

D effective product layer diffusivity of CO_2 (m^2/s)

D_o pre-exponential factor of the effective diffusion coefficient (m^2/s)

$Ea_{K,\,D,\,R}$ activation energy for the kinetic regime, K; for the combined diffusion and kinetic regime D; and R, for the recarbonation reaction Equations (5) and (6) (kJ/mol)

$h_{,\,K\text{-}D,\,D,max}$ critical product layer thickness (m) marking the transition between kinetic and diffusion reaction regimes (K-D); the end of the diffusion regime (D): ot the the end of the fast reaction period in the carbonator (max)

k sorbent deactivation constant

$k_{s0,R}$ pre-exponential factor for the recarbonation rate constant in Equation (5) in (m^4/kmols) or in (s^{-1}) according to Equation (6)

$k_{s,R}$ apparent kinetic constant of the recarbonation reaction in Equation (5) in (m^4/kmols) or in (s^{-1}) according to Equation (6)

k_{so} pre-exponential factor for the reaction rate constant according to RPM (m^4/kmols)

k_s reaction rate constant for the surface reaction according to the RPM (m^4/kmols)

L total length of pore system (m/m^3)

$M_{CaO,\ CaCO3}$ molecular weight of CaO; of $CaCO_3$ (kg/kmol)

N total number of calcination cycles

R number of calcination-carbonation-recarbonation cycles

S specific reaction surface (m^2/m^3)

$S_{N,R}$ reaction surface for cycle N after R recarbonations (m^2/m^3)

$S_{N,R\ av}$ reaction surface available for recarbonation (m^2/m^3)

t time (s)

$V^M_{CaO,\ CaCO3}$ molar volumes of CaO; of $CaCO_3$ (m^3/kmol)

X CaO carbonate molar conversion

X_N CO_2 carrying capacity of CaO after N calcination-carbonation cycles

$X_{N,R}$ CO_2 carrying capacity of CaO after N calcination-carbonation cycles that include R cycles with a recarbonation stage after carbonation within the last cycles

$X_{N,R}^{+}$ CaO carbonate molar conversion achieved at the end of the fast recarbonation period after N calcination-carbonation and R recarbonation cycles

X_{K-D} CaO carbonate molar conversion in the transition between kinetic and diffusion reaction regimes

X_r CaO carbonate molar conversion for very large cycle numbers N, or residual CO_2 carrying capacity of CaO

Z ratio of volume of product solid phase after reaction and before reaction

Greek Letters

β parameter from RPM model that refers to the contribution of the chemical reaction and the CO_2 apparent diffusion coefficient through the product layer to the reaction rate

ΔX_R increase in the CaO carbonate molar conversion attained due to recarbonation

$\Delta X_{R,max}$ maximum increase in the CaO carbonate molar conversion attained during the fast recarbonation period

ε porosity

Ψ	sorbent structural parameter from the RPM model
$\rho_{CaO,CaCO3}$	density of CaO; of $CaCO_3$ (kg/m^3)
τ	parameter from the RPM model referring to non dimensional time
$\boldsymbol{\vartheta}$	volume fraction of CO_2

Acknowledgements

This work is supported by the European Programme of the Research Fund for Coal and Steel under RECaL project (RFCR-CT-2012-00008). Financial support for I. Martínez during her PhD studies has been provided by the FPU programme of the Spanish Ministry of Education (AP2009-3575). M.E. Diego acknowledges a fellowship grant under the CSIC JAE Programme, co-funded by the European Social Fund.

References

1. Metz, B.; Davidson, O.; de Coninck, H.; Loos, M.; Meyer, L. *IPCC Special Report on Carbon Dioxide Capture and Storage. Prepared by Working Group III of the Intergovernmental Panel on Climate Change*; Cambridge University Press, Cambridge, United Kingdom and New York, NY, USA, 2005; p 442.

2. Shimizu, T.; Hirama, T.; Hosoda, H.; Kitano, K.; Inagaki, M.; Tejima, K., A Twin Fluid-Bed Reactor for Removal of CO_2 from Combustion Processes. *Chemical Engineering Research and Design* 1999, 77, (1), 62-68.

3. Abanades, J. C.; Anthony, E. J.; Lu, D. Y.; Salvador, C.; Alvarez, D., Capture of CO_2 from combustion gases in a fluidized bed of CaO. *AIChE Journal* 2004, 50, (7), 1614-1622.

4. Alonso, M.; Rodríguez, N.; González, B.; Grasa, G.; Murillo, R.; Abanades, J. C., Carbon dioxide capture from combustion flue gases with a calcium oxide chemical loop. Experimental results and process development. *International Journal of Greenhouse Gas Control* 2010, 4, (2), 167-173.

5. Charitos, A.; Hawthorne, C.; Bidwe, A. R.; Sivalingam, S.; Schuster, A.; Spliethoff, H.; Scheffknecht, G., Parametric investigation of the calcium looping process for CO_2 capture in a 10 kW_{th} dual fluidized bed. *International Journal of Greenhouse Gas Control* 2010, 4, (5), 776-784.

6. Rodríguez, N.; Alonso, M.; Abanades, J. C., Experimental investigation of a circulating fluidized-bed reactor to capture CO_2 with CaO. *AIChE Journal* 2011, 57, (5), 1356-1366.

7. Charitos, A.; Rodríguez, N.; Hawthorne, C.; Alonso, M.; Zieba, M.; Arias, B.; Kopanakis, G.; Scheffknecht, G.; Abanades, J. C., Experimental validation of the calcium looping CO_2 capture

process with two circulating fluidized bed carbonator reactors. *Industrial and Engineering Chemistry Research* 2011, 50, (16), 9685-9695.

8. Galloy, A.; Bayrak, A.; Kremer, J.; Orth, M.; Plötz, S.; Wieczorek, M.; Zorbach, I.; Ströhle, J.; Epple, B., CO_2 Capture in a 1 MW_{th} Fluidized Bed Reactor in Batch Mode Operation. In *Fifth International Conference on Clean Coal Technologies, IEA*, Zaragoza (Spain), 2011.

9. Kremer, J.; Galloy, A.; Ströhle, J.; Epple, B., Continuous CO_2 Capture in a 1-MWth Carbonate Looping Pilot Plant. *Chemical Engineering Technology* 2013, 36, (9), 1518-1524.

10. Dieter, H.; Hawthorne, C.; Zieba, M.; Scheffknecht, G., Progress in Calcium Looping Post Combustion CO_2 Capture: Successful Pilot Scale Demonstration. *Energy Procedia* 2013, 37, 48-56.

11. Sánchez-Biezma, A.; Ballesteros, J. C.; Diaz, L.; de Zárraga, E.; Álvarez, F. J.; López, J.; Arias, B.; Grasa, G.; Abanades, J. C., Postcombustion CO_2 capture with CaO. Status of the technology and next steps towards large scale demonstration. *Energy Procedia* 2011, 4, 852-859.

12. Arias, B.; Diego, M. E.; Abanades, J. C.; Lorenzo, M.; Diaz, L.; Martínez, D.; Alvarez, J.; Sánchez-Biezma, A., Demonstration of steady state CO_2 capture in a 1.7 MW_{th} calcium looping pilot. *International Journal of Greenhouse Gas Control* 2013, 18, 237-245.

13. Martínez, I.; Murillo, R.; Grasa, G.; Carlos Abanades, J., Integration of a Ca looping system for CO_2 capture in existing power plants. *AIChE Journal* 2011, 57, (9), 2599-2607.

14. Romano, M., Coal-fired power plant with calcium oxide carbonation for post-combustion CO_2 capture. *Energy Procedia* 2009, 1, 1099-1106.

15. Romeo, L. M.; Abanades, J. C.; Escosa, J. M.; Paño, J.; Giménez, A.; Sánchez-Biezma, A.; Ballesteros, J. C., Oxyfuel carbonation/calcination cycle for low cost CO_2 capture in existing power plants. *Energy Conversion and Management* 2008, 49, (10), 2809-2814.

16. Ströhle, J.; Lasheras, A.; Galloy, A.; Epple, B., Simulation of the carbonate looping process for post-combustion CO_2 capture from a coal-fired power plant. *Chemical Engineering and Technology* 2009, 32, (3), 435-442.

17. Curran, G. P.; Fink, C. E.; Gorin, E., Carbon dioxide-acceptor gasification process: studies of acceptor properties. *Advanced Chemistry Services* 1967, 69, 141-165.

18. Barker, R., The reversibility of the reaction $CaCO_3 \rightleftarrows CaO+CO_2$. *Journal of Applied Chemistry and Biotechnology* 1973, 23, (10), 733-742.

19. Silaban, A.; Harrison, D. P., High-temperature capture of carbon dioxide: characteristics of the reversible reaction between CaO(s) and CO_2(g). *Chemical Engineering Communications* 1995, 137, 177-190.

20. Abanades, J. C.; Alvarez, D., Conversion limits in the reaction of CO_2 with lime. *Energy and Fuels* 2003, 17, (2), 308-315.

21. Abanades, J. C., The maximum capture efficiency of CO_2 using a carbonation/calcination cycle of $CaO/CaCO_3$. *Chemical Engineering Journal* 2002, 90, (3), 303-306.

22. Abanades, J. C.; Rubin, E. S.; Anthony, E. J., Sorbent cost and performance in CO_2 capture systems. *Industrial and Engineering Chemistry Research* 2004, 43, (13), 3462-3466.

23. Lisbona, P.; Martínez, A.; Lara, Y.; Romeo, L. M., Integration of carbonate CO_2 capture cycle and coal-fired power plants. A comparative study for different sorbents. *Energy and Fuels* 2010, 24, (1), 728-736.

24. Anthony, E. J., Solid Looping Cycles: A New Technology for Coal Conversion. *Industrial & Engineering Chemistry Research* 2008, 47, (6), 1747-1754.

25. Blamey, J.; Anthony, E. J.; Wang, J.; Fennell, P. S., The calcium looping cycle for large-scale CO_2 capture. *Progress in Energy and Combustion Science* 2010, 36, (2), 260-279.

26. Arias, B.; Grasa, G.; Alonso, M.; Abanades, J. C., Post-combustion calcium looping process with a highly stable sorbent activity by recarbonation. *Energy & Environmental Science* 2012, 5, 7353-7359.

27. Lysikov, I.; Salanov, N.; Okunev, G., Change of CO2 Carrying Capacity of CaO in Isothermal Recarbonation-Decomposition Cycles. *Industrial & Engineering Chemistry Research* 2007, 46, (13), 4633-4638.
28. Sun, P.; Lim, C. J.; Grace, J. R., Cyclic CO2 Capture by Limestone- Derived Sorbent During Prolonged Calcination/Carbonation Cycling. *AIChE Journal* 2008, 54, (6), 1668-1677.
29. Grasa, G. S.; Abanades, J. C., CO_2 capture capacity of CaO in long series of carbonation/calcination cycles. *Industrial and Engineering Chemistry Research* 2006, 45, (26), 8846-8851.
30. Dennis, J. S.; Pacciani, R., The rate and extent of uptake of CO_2 by asynthetic, CaO-containing sorbent. *Chemical Engineering Science* 2009, 64, (9), 2147-2157.
31. Arias, B.; Abanades, J. C.; Grasa, G. S., An analysis of the effect of carbonation conditions on CaO deactivation curves. *Chemical Engineering Journal* 2011, 167, (1), 255-261.
32. Salvador, C.; Lu, D.; Anthony, E. J.; Abanades, J. C., Enhancement of CaO for CO2 capture in FBC environment. *Chemical Engineering Journal* 2003, 96, 187-195.
33. Bhatia, S. K.; Perlmutter, D. D., Effect of the product layer on the kinetics of the CO_2-lime reaction. *AIChE Journal* 1983, 29, (1), 79-86.
34. Mess, D.; Sarofim, A. F.; Longwell, J. P., Product Layer Diffusion during the Reaction of Calcium Oxide with Carbon Dioxide. *Energy & Fuels* 1999, 13, (5), 999-1005.
35. Stanmore, B. R.; Gilot, P., Review—calcination and carbonation of limestone during thermal cycling for CO2 sequestration. *Fuel Processing Technology* 2005, 86, 1707-1743.
36. Bouquet, E.; Leyssens, G.; Schönnenbeck, C.; Gilot, P., The decrease of carbonation efficiency of CaO along calcination–carbonation cycles: Experiments and modelling. *Chemical Engineering Science* 2009, 64, (9), 2136-2146.
37. Stendardo, S.; Foscolo, P. U., Carbon dioxide capture with dolomite: A model for gas-solid reaction within the grains of a particulate sorbent. *Chemical Engineering Science* 2009, 64, (10), 2343-2352.
38. Liu, W.; Dennis, J. S.; Sultan, D. S.; Redfern, S. A. T.; Scott, S. A., An investigation of the kinetics of CO_2 uptake by a synthetic calcium based sorbent. *Chemical Engineering Science* 2012, 69, (1), 644-658.
39. Sun, P.; Grace, J. R.; Lim, C. J.; Anthony, E. J., A discrete-pore-size-distribution-based gas–solid model and its application to the reaction. *Chemical Engineering Science* 2008, 63, (1), 57-70.
40. Alvarez, D.; Abanades, J. C., Determination of the critical product layer thickness in the reaction of CaO with CO2. *Industrial & Engineering Chemistry Research* 2005, 44, (15), 5608-5615.
41. Grasa, G.; Murillo, R.; Alonso, M.; Abanades, J. C., Application of the random pore model to the carbonation cyclic reaction. *AIChE Journal* 2009, 55, (5), 1246-1255.
42. Sun, P.; Grace, J. R.; Lim, C. J.; Anthony, E. J., Determination of intrinsic rate constants of the CaO–CO_2 reaction. *Chemical Engineering Science* 2008, 63, (1), 47-56.
43. Li, Z.; Fang, F.; Tang, X.; Cai, N., Effect of Temperature on the Carbonation Reaction of CaO with CO_2. *Energy & Fuels* 2012, 26, (4), 2473-2482.
44. Arias, B.; Grasa, G.; Abanades, J. C.; Manovic, V.; Anthony, E. J., The Effect of Steam on the Fast Carbonation Reaction Rates of CaO. *Industrial & Engineering Chemistry Research* 2012, 51, (5), 2478-2482.
45. Manovic, V.; Anthony, E. J., Carbonation of CaO-Based Sorbents Enhanced by Steam Addition. *Industrial & Engineering Chemistry Research* 2010, 49, (19), 9105-9110.

46. Alonso, M.; Rodríguez, N.; Grasa, G.; Abanades, J. C., Modelling of a fluidized bed carbonator reactor to capture CO_2 from a combustion flue gas. *Chemical Engineering Science* 2009, 64, (5), 883-891.

47. Romano, M. C., Modeling the carbonator of a Ca-looping process for CO2 capture from power plant flue gas. *Chemical Engineering Science* 2012, 69, (1), 257-269.

48. Lasheras, A.; Ströhle, J.; Galloy, A.; Epple, B., Carbonate looping process simulation using a 1D fluidized bed model for the carbonator. *International Journal of Greenhouse Gas Control* 2011, 5, (4), 686-693.

49. Ylätalo, J.; Ritvanen, J.; Arias, B.; Tynjälä, T.; Hyppänen, T., 1-Dimensional modelling and simulation of the calcium looping process. *International Journal of Greenhouse Gas Control* 2012, 9, 130-135.

50. Grasa, G. S.; Abanades, J. C.; Alonso, M.; González, B., Reactivity of highly cycled particles of CaO in a carbonation/calcination loop. *Chemical Engineering Journal* 2008, 137, (3), 561-567.